Electronic Supplementary Information

Extensive Reference Set and Refined Computational Protocol for Calculations of ^{57}Fe Mössbauer Parameters

Golokesh Santra, Frank Neese, Dimitrios A. Pantazis

Max-Planck-Institut für Kohlenforschung, Kaiser-Wilhelm-Platz 1, 45470 Mülheim an der Ruhr, Germany

Table S1: Molecular Iron Complexes present in the MPMIC80 dataset.

	Complex[a]	$2S+1$[b]	Fe ox.	δ_{exp} (mm s^{-1})	$\lvert\Delta E_Q\rvert_{exp}$ (mm s^{-1})	T (K)	Refs.
1	$[Fe(CO)_4H]^-$	1	0	-0.17	1.36	77	1
2	$[Fe(CO)_5]$	1	0	-0.18	2.57	4.2	2, 3
3	[Fe(η4-butadiene)$(CO)_3$]	1	0	0.12	1.34	78	4
4	$Fe(CO)_3$(cyclo-butadiene)	1	0	0.02	1.52	78	5
5	$(^{Me}L^{Me,Me})Fe(CNXyl)_3$	2	1	0.17	0.81	80	6
6	$L^{Me}Fe(\eta^6\text{-}C_6H_6)$	2	1	0.70	0.74	80	6
7	$(^{Me}L^{Me,Me})Fe(CO)_3$	2	1	0.12	0.77	80	6
8	$Fe(phen)_2(NCS)_2$ (LS)	1	2	0.34	0.34	77	7, 8
9	$Fe(LN_4)(NCS)_2$ (LS)	1	2	0.44	0.77	80	9
10	Fc (Ferrocene)	1	2	0.53	2.40	80	10
11	$[Fe(pyS_4)(PH_3)]$	1	2	0.34	0.69	80	11
12	$[Fe(pyS_4)(CO)]$	1	2	0.19	0.88	80	11
13	$CpFe(CO)_2Cl$	1	2	0.27	1.82	4.2	12
14	[Fe(OEP)(CO)]	1	2	0.27	1.84	4.2	13
15	$[Fe(PyO)I(CO)_2PPh_3]$	1	2	0.10	0.48	55	14
16	$[Fe(PyS)I(CO)_2PPh_3]$	1	2	0.10	0.35	77	15
17	$CpFe(CO)_2Me$	1	2	0.08	1.76	78	16
18	$[\{Fe\text{–}NO\}^6(pyS_4)]^+$	1	2	0.04	1.63	80	11
19	$[CpFe(CO)_3]^+$	1	2	0.05	1.88	78	10
20	$[Fe(bipy)_3]^{2+}$	1	2	0.33	0.39	77	17
21	$[Fe(phen)_3]^{2+}$	1	2	0.34	0.23	77	18
22	$\{Fe[HC(3,5\text{-}Me_2pz)_3]_2\}I_2$ (LS)	1	2	0.46	0.21	4.2	19
23	$Fc(COOH)_2$	1	2	0.48	2.16	80	20
24	$[Fe(pyS_4)(SMe_3)]$	1	2	0.44	0.43	80	11
25	$PcFePy_2$	1	2	0.32	1.96	4.2	21
26	$[Fe(SC_5H_4NCO)I(CO)_2(ArNC)]$	1	2	0.01	0.29	77	15
27	$[(TIMMN_{Mes})Fe(NAd)]$	1	2	-0.18	0.41	80	22
28	FcC≡CH	1	2	0.52	2.34	80	23
29	FcCN	1	2	0.52	2.36	80	10
30	Fc(COMe)	1	2	0.54	2.27	80	20
31	$Fc(COMe)_2$	1	2	0.49	2.27	80	20
32	$Fc(CO_2Me)$	1	2	0.53	2.30	80	20
33	$Fc(CO_2Me)_2$	1	2	0.54	2.34	80	20
34	$[\{Fe\text{-}NO\}^7(PyS_4)]$	2	2	0.33	0.40	80	11
35	[Fe(OEP)]	3	2	0.62	1.71	4.2	24
36	[Fe(TPP)]	3	2	0.52	1.51	4.2	25, 26
37	$Fe(phen)_2(NCS)_2$ (HS)	5	2	1.01	2.82	77	7, 8
38	$Fe(cis\text{-}phen)_2Cl_2$	5	2	1.08	3.26	80	27
39	$[Fe(LN_4)(NCS)_2]$ (HS)	5	2	1.11	2.51	80	9
40	$[FeS_4C_8O_4]^{2-}$	5	2	0.67	4.01	4.2	28
41	$[Fe(SPh)_4]^{2-}$	5	2	0.66	3.24	4.2	28
42	$[Fe(NCS)_4]^{2-}$	5	2	0.97	2.83	4.2	29
43	$[Fe(SR)_3]^-$; R=C_6H_2-2,4,6-tBu_3	5	2	0.56	0.83	4.2	30, 31
44	$[Fe(CH_3CO_2)TPpivP]^-$	5	2	1.05	4.25	4.2	32
45	$(^{Me}L^{Me,Me})_2Fe$	5	2	0.84	1.80	80	33
46	$[Fe(bipy)_3]^{3+}$	2	3	0.07	1.76	77	34
47	$[Fe(phen)_3]^{3+}$	2	3	0.10	1.67	77	18
48	$[Fe(terpy)_2]^{3+}$	2	3	0.08	3.32	4.2	35, 36
49	$[Fe\text{-}trans\text{-}(cyclam)(N_3)_2]^-$	2	3	0.29	2.24	80	37
50	$[Fe(OEP)(4\text{-}NMe_2Py)]^+$	2	3	0.26	2.15	4.2	38
51	$[Fe(acpa)_2]^-$ (LS)	2	3	0.25	2.24	78	39
52	Fe(thpu)(Hthpu) (LS)	2	3	0.28	3.09	80	40
53	$[(TIMMN_{Mes})Fe(NAd)]^+$	2	3	-0.12	2.54	80	22
54	$[Cp^*_2Fe]^+$	2	3	0.57	0.00	77	41
55	$Fe(mnt)_2(idzm)$	4	3	0.36	2.64	77	42
56	$[Fe(\eta4\text{-}MAC^*)Cl]^{2-}$	4	3	0.25	3.60	4.2	43

57	$[Fe(S\text{-}t\text{-}Bu)_3NO]^-$	4	3	0.26	0.46	4.2	44
58	$[Fe(SEt)_4]^-$	6	3	0.25	0.62	4.2	45
59	$[Fe(NO)_2(S(p\text{-}Me)Ph)]^{2-}$	6	3	0.18	0.69	4.2	46
60	$[Fe(C_{33}H_{37}N_4)Cl]$	6	3	0.39	1.36	70	47
61	$[Fe(porphyrin)(CH_3COO)]$	6	3	0.40	1.10	4.2	48
62	$Fe(acac)_3$	6	3	0.53	0.64	78	49
63	$Fe(tfa)_3$	6	3	0.53	0.67	78	49
64	$[Fe(phen)_2Cl_2]^+$	6	3	0.39	0.05	80	10
65	PcFeCl	6	3	0.28	2.56	77	21
66	$(^{Me}L^{Me,Me})FeCl_2$	6	3	0.33	1.23	80	50
67	$[Cp^*_2Fe(CO)]^{2+}$	1	4	0.42	3.22	77	41
68	$[(TIMMN^{Mes})Fe(NAd)]^{2+}$	1	4	-0.14	3.54	80	22
69	$[(N_3N')Fe(CN)]$	1	4	-0.20	3.22	80	51
70	$Fe(PPh_3)2(\text{“}S2\text{”})_2$	3	4	0.16	1.52	4.2	52
71	$Fe(PPh_3)(\text{“}S2\text{”})_2$	3	4	0.12	3.03	4.2	52
72	$[Fe(N_4Py)(O)]^{2-}$	3	4	-0.04	0.93	4.2	53
73	$[Fe(O)(TMC)(NCCH_3)]^{2+}$	3	4	0.17	1.24	4.2	54
74	$[Cp^*_2Fe]^{2+}$	3	4	0.59	2.00	77	41
75	$[Fe(O)(porphyrin)]^+$	4	4	0.08	1.62	4.2	55
76	$[Fe(\eta4\text{-}MAC^*)Cl]^-$	5	4	0.04	0.89	4.2	56
77	$[Fe(B^*)(O)]^-$	2	5	-0.42	4.25	4.2	57
78	$[Fe(cyclam\text{-}acetate)(N)]^+$	2	5	-0.02	1.60	80	58
79	$[Fe(Me_3cyclam\text{-}acetate)(N)]^{2+}$	1	6	-0.29	1.53	4.2	59
80	$[(TIMMN^{Mes})Fe(N)(F)]^{3+}$	2	7	-0.72	3.30	78	60

[a]LS= low-spin; HS= high-spin; Pc= phthalocyanine; $^{Me}L^{Me,Me}$ = methyl substituted β-diketiminate; CNXyl = 2,6-dimethylphenyl isocyanide; Cp= cyclopentadiene; PyO= 6-methyl-2-pyridonate; PyS=, 6-methyl-pyridyl-2-thiolate; pyS_4= dianion of 2,6-bis(2-mercaptophenylthiomethyl)pyrdidine; TMC= 1,4,8,11-tetramethyl-1,4,8,11-tetraazacyclotetradecane; OEP= dianion of octaethylporphyrin; bipy= 2,2′-bipyridine; phen= 1,10-phenanthroline; Pz= Pyrazole; ArNC= 2,6-Me_2-C_6H_3NC; TPP= tetraphenylporphyrinate; $TIMMN_{Mes}$= tris-[2-(3-mesityl-imidazole-2-ylidene)-methyl]amine; Ad= adamantane; Hacpa = N−(1-acetyl-2-propylidene)(2-pyridylmethyl)amine; H_2thpu= Pyruvic acid thiosemicarbazone; Cp*= Pentamethylcyclopentadien; mnt = cis-1,2-dicyano-1,2-ethylenedithiolato; idzm =2-(p-pyridyl)-4,4,5,5-tetramethylimidazolinium; acac= acetylacetonate; tfa= trifluoroacetylacetonate; MAC* = tetra-anion of 1,4,8,11-tetraaza-13,13-diethyl-2,2,5,5,7,7,10,10-octamethyl-3,6,9,12,14-pentaoxocyclotetradecane; “S2” = 1,2-benzenedithiolato-S,S′ dianion; B* = tetra-anion of 3,3,6,6,9,9-hexamethyl-3,4,8,9-tetrahydro-1H-1,4,8,11-benzotetraazacyclotridecine-2,5,7,10(6H,11H)-tetraone. N_3N'= tris(N-trimethylsilyl-2-amidoethyl)amine ligand; terpy= 2,2′:6′2″-terpyridine; LN_4= N-[(1-H-imidazol-4-yl)methylene]-N′-(1-pyridin-2-yl-ethylidene)-2,2-dimethyl-propane-1,3-diamin; TPpivP= “pivalamide-picket-fence” porphyrin; cyclam= 1,4,8,11-tetraazacyclotetradecane;

[b]Total spin multiplicity of the complex.

Table S2: 21 molecular iron complexes and their experimental isomer shifts present in the high-T subset. The experimental isomer shifts were recorded at room temperature or close.

	Complex[a]	$2S+1$[b]	Fe ox. state	δ_{exp} (mm s^{-1})	Refs.
1	$PcFe(_iPrNH_2)_2$	1	2	0.25	61
2	$PcFe(dabco)_2$	1	2	0.33	61
3	$PcFe(Pz)_2$	1	2	0.26	61
4	$PcFe(THT)_2$	1	2	0.27	61
5	PcFe(CO)(Py)	1	2	0.11	61
6	$PcFe(CO)(NH_3)$	1	2	0.12	61
7	$PcFe(PEt_3)_2$	1	2	0.16	61
8	$PcFe(Et_2NH)_2$	1	2	0.25	61
9	$PcFe(MeIm)_2$	1	2	0.24	61
10	$PcFe(Iz)_2$	1	2	0.27	61
11	$PcFe(Pyr)_2$	1	2	0.24	61
12	$PcFe(Tetr)_2$	1	2	0.15	61
13	PcFe(CO)(THF)	1	2	0.10	61
14	PcFe(CO)(Pip)	1	2	0.11	61
15	$PcFe(P(OEt)_3)_2$	1	2	0.13	61
16	$Fc(CO_2H)$	1	2	0.44	20
17	$PcFe(mepip)_2$	1	2	0.27	21
18	$\{Fe[HC(3,5\text{-}Me_2pz)_3]_2\}I_2$ (HS)	5	2	0.97	62
19	$[Fe(acpa)_2]^+$ (HS)	6	3	0.33	39
20	Fe(thpu)(Hthpu) (HS)	6	3	0.47	40
21	$[Fe(bipy)_2Cl_2]^+$	6	3	0.42	23

[a]HS= high-spin; Pc= phthalocyanine; dabco= 1,4-diazabicyclo[2.2.2]octane; Pz= Pyrazole; THT=tetrahydrothiophene; MeIm= N-methylimidazole; Iz= isoxazole; Tetr= tetrazine; THF= tetrahydrofuran; Pip= piperidine; mepip= 4-methylpiperidine; Hacpa = N−(1-acetyl-2-propylidene)(2-pyridylmethyl)amine; H_2thpu= Pyruvic acid thiosemicarbazone; bipy= 2,2′-bipyridine.

[b]Total spin multiplicity of the complex.

Table S3: Bond length and angles relevant to the Fe centre of two selected complexes. The structures are optimized by employing Defgrid2 and Defgrid3 integration grids and TPSSh-D3BJ/X2C/x2c-TZVPall method.

Complex #09 [Fe^{II}; 2S+1=1]			Complex #57 [Fe^{III}; 2S+1=4]		
Bond lengths (Å) & Bond angles (°)	**Defgrid2**	**Defgrid3**	**Bond lengths (Å) & Bond angles (°)**	**Defgrid2**	**Defgrid3**
Fe_1-N_4	1.939	1.939	**Fe_1-S_2**	2.264	2.264
Fe_1-N_5	2.017	2.017	**Fe_1-S_3**	2.280	2.280
Fe_1-N_6	1.918	1.918	**Fe_1-S_4**	2.270	2.270
Fe_1-N_7	1.936	1.936	**Fe_1-N_6**	1.705	1.705
Fe_1-N_8	1.938	1.938	**N_6-O_5**	1.179	1.179
Fe_1-N_9	1.950	1.950			
∠N_9-Fe_1-N_4	85.2	85.1	**∠Fe_1-N_6-O_5**	174.0	174.0
∠N_9-Fe_1-N_5	84.5	84.5	**∠S_2-Fe_1-N_6**	103.5	103.6
∠N_9-Fe_1-N_6	101.4	101.4	**∠S3-Fe_1-N_6**	113.2	113.2
∠N_9-Fe_1-N_7	89.0	89.0	**∠S_4-Fe_1-N_6**	112.8	112.7
∠N_8-Fe_1-N_4	93.5	93.4			
∠N_8-Fe_1-N_5	90.2	90.2			
∠N_8-Fe_1-N_6	84.1	84.1			
∠N_8-Fe_1-N_7	92.8	92.8			
∠Fe_1-N_8-C_{52}	147.2	147.2			
∠Fe_1-N_9-C_{51}	142.4	142.4			
∠N_9-Fe_1-N_8	174.1	174.1			

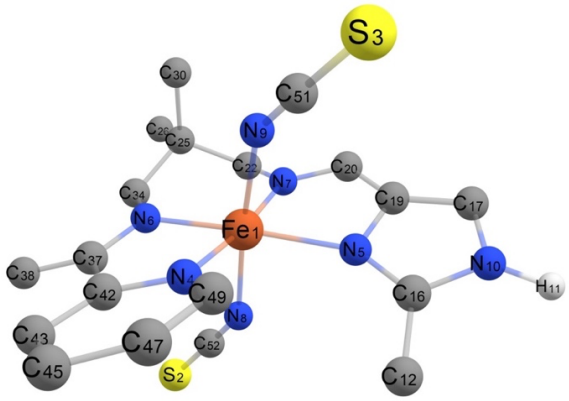

Complex #09

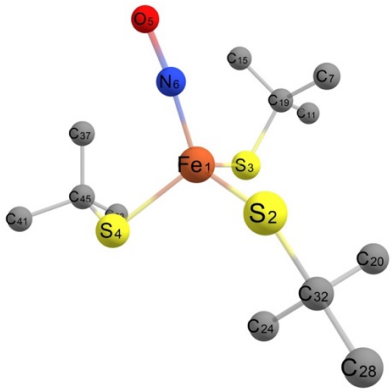

Complex #57

Table S4: Calibration constants and statistical parameters obtained by fitting $\delta_{exp} = \{a[\rho(0) - C] + b\}$ for different basis sets of Fe. The calculations were performed using B3LYP functional, point nucleus model, and first order picture change effect.[a]

Basis set for Fe	***a***	***b***	**C**	**R^2**	**MAD[b] (mm s^{-1})**	**Max. Dev.[c] (mm s^{-1})**	**St. Dev.[d] (mm s^{-1})**
CP(PPP)	–0.30	1.1422	14398	0.951	0.056	0.201	0.074
x2c-TZVPPall	–0.22	0.9337	13652	0.813	0.112	0.347	0.144
x2c-TZVPPall-s	–0.21	0.9939	13652	0.789	0.120	0.369	0.153
aug-cc-pVTZ-J	–0.55	1.3429	7762	0.942	0.060	0.228	0.080
DKH-def2-TZVPP	–0.30	1.0041	14078	0.939	0.063	0.208	0.082
ANO-RCC-VTZP	–0.18	0.9043	15626	0.416	0.185	0.730	0.255
s-decontracted x2c-TZVPPall	–0.31	1.0685	13695	0.943	0.059	0.195	0.080
s-decontracted aug-cc-pVTZ-J	–0.26	1.1819	16644	0.943	0.060	0.212	0.080
s-decontracted aug-cc-pVTZ-J (-*dfg*)	–0.26	1.2129	16644	0.951	0.057	0.214	0.074
aug-cc-pVTZ-Jmod[63]	–0.28	1.0331	14943	0.943	0.060	0.212	0.080

[a] *a* and *b* are the fitting coefficients obtained from the fit of $\delta_{exp} = \{a[\rho(0) - C] + b\}$. C is a constant, which is very close to the calculated $\rho(0)$ value. The units of *a, b,* and C are a.u.^{3} mm s^{-1}, mm s^{-1}, and a.u.$^{-3}$, respectively. R^2 is the coefficient of determination from the linear fit.

[b]Mean absolute deviations of the calculated ISs with respect to the experimental ISs, where the former ones are obtained by using $\delta_{exp} = \{a[\rho(0) - C] + b\}$.

[c]Maximum deviation of the calculated ISs from the experimental ISs.

[d]Standard deviation of the calculated ISs.

Table S5: Calibration constants and statistical parameters from the linear regression analysis of the computed contact densities using different DFT functionals and the experimental isomer shifts using.[a] The *s*-decontracted aug-cc-pVTZ-J(-*dfg*) basis set was employed across the board for Fe.

Methods	***a***	***b***	**C**	**R^2**	**MAD[b] (mm s^{-1})**	**Max. Dev.[c] (mm s^{-1})**	**St. Dev.[d] (mm s^{-1})**
SVWN5	-0.32	0.8909	14831	0.913	0.071	0.296	0.098
BP86	-0.32	0.9924	14960	0.922	0.067	0.270	0.093
PBE	-0.31	0.9936	14933	0.920	0.067	0.267	0.094
BLYP	-0.32	1.0945	14954	0.917	0.070	0.274	0.096
TPSS	-0.32	1.0013	14917	0.935	0.060	0.243	0.085
PBE0	-0.28	1.1199	14920	0.965	0.050	0.149	0.063
B1LYP	-0.28	1.1340	14936	0.961	0.054	0.151	0.066
B3LYP	-0.29	1.1051	14930	0.958	0.053	0.181	0.069
TPSSh	-0.30	1.1945	14913	0.954	0.052	0.228	0.072
TPSS0	-0.28	1.1402	14908	0.968	0.048	0.123	0.060
M06	-0.31	0.9414	15010	0.936	0.065	0.278	0.084
LC-BLYP	-0.29	1.0826	14951	0.950	0.062	0.169	0.075
CAM-B3LYP	-0.27	1.2037	14939	0.958	0.056	0.138	0.068
ωB97X	-0.27	1.1675	15034	0.958	0.055	0.147	0.068
B2PLYP	-0.24	1.1366	14916	0.939	0.066	0.182	0.082

[a] *a* and *b* are the fitting coefficients obtained from the fit of $\delta_{exp} = \{a[\rho(0) - C] + b\}$. C is a constant, which is very close to the calculated ρ(0) value. The units of *a, b,* and C are a.u.^{3} mm s^{-1}, mm s^{-1}, and a.u.$^{-3}$, respectively. R^2 is the coefficient of determination from the linear fit.

[b]Mean absolute deviations of the calculated ISs with respect to the experimental ISs, where the former ones are obtained by using $\delta_{exp} = \{a[\rho(0) - C] + b\}$.

[c]Maximum deviation of the calculated ISs from the experimental ISs.

[d]Standard deviation of the calculated ISs.

Table S6: Calibration constants and statistical parameters from the linear regression analysis of the computed contact densities using different DFT functionals with varying %HF exchange and the experimental isomer shifts.[a]

Functionals	*a*	*b*	C	R^2	MAD[b] (mm s^{-1})	Max. Dev.[c] (mm s^{-1})	St. Dev.[d] (mm s^{-1})
BLYP	–0.32	1.0974	14954	0.917	0.070	0.275	0.096
B10LYP	–0.30	1.0647	14947	0.942	0.059	0.227	0.080
B1LYP	–0.28	1.1358	14936	0.961	0.054	0.150	0.066
B30LYP	–0.27	1.2415	14932	0.961	0.054	0.140	0.066
BH&HLYP	–0.24	1.1259	14918	0.942	0.064	0.175	0.080
B70LYP	–0.22	1.0230	14904	0.910	0.081	0.236	0.100
TPSS	–0.32	1.0045	14917	0.935	0.060	0.243	0.085
TPSSh	–0.30	1.1976	14913	0.954	0.052	0.227	0.072
TPSS0	–0.28	1.1425	14908	0.967	0.049	0.122	0.060
TPSS30	–0.27	1.2122	14906	0.966	0.050	0.131	0.062
TPSS50	–0.24	1.2125	14899	0.945	0.064	0.185	0.078
TPSS70	–0.22	1.2021	14892	0.912	0.080	0.263	0.099

[a] *a* and *b* are the fitting coefficients obtained from the fit of $\delta_{exp} = \{a[\rho(0) - C] + b\}$. C is a constant, which is very close to the calculated ρ(0) value. The units of *a, b,* and C are a.u.^{3} mm s^{-1}, mm s^{-1}, and a.u.$^{-3}$, respectively. R^2 is the coefficient of determination from the linear fit.

[b]Mean absolute deviations of the calculated ISs with respect to the experimental ISs, where the former ones are obtained by using $\delta_{exp} = \{a[\rho(0) - C] + b\}$.

[c]Maximum deviation of the calculated ISs from the experimental ISs.

[d]Standard deviation of the calculated ISs.

Table S7: Calibration constants and statistical parameters from the linear regression analysis of the B2PLYP/*s*-decontracted aug-cc-pVTZ-J (Fe) level contact densities against the experimental isomer shifts with unrelaxed and relaxed PT2 density.[a]

PT2 density	*a*	*b*	C	R^2	MAD[b] (mm s^{-1})	Max. Dev.[c] (mm s^{-1})	St. Dev.[d] (mm s^{-1})
Unrelaxed	-0.24	1.1367	14916	0.939	0.066	0.183	0.083
Relaxed	-0.27	1.2174	14916	0.916	0.072	0.306	0.096

[a] *a* and *b* are the fitting coefficients obtained from the fit of $\delta_{exp} = \{a[\rho(0) - C] + b\}$. C is a constant, which is very close to the calculated ρ(0) value. The units of *a, b,* and C are a.u.^{3} mm s^{-1}, mm s^{-1}, and a.u.$^{-3}$, respectively. R^2 is the coefficient of determination from the linear fit.

[b]Mean absolute deviations of the calculated ISs with respect to the experimental ISs, where the former ones are obtained by using $\delta_{exp} = \{a[\rho(0) - C] + b\}$.

[c]Maximum deviation of the calculated ISs from the experimental ISs.

[d]Standard deviation of the calculated ISs.

Table S8: For ten different basis sets, the mean absolute deviations (MADs) and root-mean-square deviations (RMSDs) of calculated quadrupole splittings with respect to the experimental values. The scalar-relativistic calculations were performed with X2C Hamiltonian, B3LYP functional, first order picture change effect, and point nucleus model.

Basis set for Fe	**MAD (mm s^{-1})**	**RMSD (mm s^{-1})**
CP(PPP)	0.308	0.447
x2c-TZVPPall	0.363	0.518
x2c-TZVPPall-s	0.316	0.455
aug-cc-pVTZ-J	0.379	0.536
DKH-def2-TZVPP	0.255	0.367
ANO-RCC-TZP	0.373	0.801
s-decontracted x2c-TZVPPall	0.387	0.515
s-decontracted aug-cc-pVTZ-J	0.373	0.520
s-decontracted aug-cc-pVTZ-J(-*dfg*)	0.373	0.520
aug-cc-pVTZ-Jmod[63]	0.351	0.494

Table S9: Performance of DFT functionals with varying fraction of HF exchange for the calculation of ^{57}Fe quadrupole splitting (ΔE_Q) values. The *s*-decontracted aug-cc-pVTZ-J(-*dfg*) basis set was employed across the board for iron.

Methods	**MAD (mm s^{-1})**	**RMSD (mm s^{-1})**
SVWN5	0.322	0.498
BP86	0.271	0.447
PBE	0.280	0.457
BLYP	0.273	0.450
TPSS	0.268	0.436
PBE0	0.377	0.526
B1LYP	0.406	0.559
B3LYP	0.349	0.489
TPSSh	0.261	0.410
TPSS0	0.384	0.524
M06	0.548	0.952
LC-BLYP	0.435	0.564
CAM-B3LYP	0.484	0.643
ωB97X	0.496	0.652
B2PLYP	0.651	0.860

Table S10: Performance of DFT functionals with varying fraction of HF exchange for the calculation of ^{57}Fe quadrupole splitting (ΔE_Q) values. The *s*-decontracted aug-cc-pVTZ-J basis set was employed for Fe.

Method	**MAD (mm s^{-1})**	**RMSD (mm s^{-1})**
BLYP	0.272	0.450
B10LYP	0.279	0.432
B1LYP	0.404	0.557
B30LYP	0.458	0.617
BHandHLYP	0.640	0.846
B69LYP	0.750	1.019
TPSS	0.269	0.437
TPSSh	0.261	0.410
TPSS0	0.383	0.525
TPSS30	0.419	0.566
TPSS50	0.601	0.793
TPSS69	0.714	0.959

Table S11: Calculated isomer shifts of nine quintet Fe^{II} and nine sextet Fe^{III} complexes using the computed ρ(0) and fitting parameters for TPSS0, B2PLYP, and DSD-PBEP86 functionals. Signed deviations and mean absolute error is reported with respect to the experimental isomer shifts.

	# Complexes in MPMIC80	δ_{exp} (mm s^{-1})	δ_{cal} (mm s^{-1})			SD(mm s^{-1})[a]		
			TPSS0	B2PLYP	DSD-PBEP86	TPSS0	B2PLYP	DSD-PBEP86
Quintet Fe^{II}	**37**	1.01	0.99	0.97	1.03	-0.02	-0.04	0.02
	38	1.08	0.96	0.95	1.02	-0.12	-0.13	-0.06
	39	1.11	1.01	1.00	1.05	-0.10	-0.11	-0.06
	40	0.67	0.66	0.62	0.67	0.00	-0.05	0.00
	41	0.66	0.67	0.62	0.66	0.01	-0.04	0.00
	42	0.97	0.92	0.90	0.95	-0.05	-0.07	-0.02
	43	0.56	0.49	0.43	0.46	-0.07	-0.13	-0.10
	44	1.05	0.96	0.94	0.99	-0.09	-0.11	-0.06
	45	0.84	0.80	0.75	0.80	-0.04	-0.09	-0.04
Sextet Fe^{III}	**58**	0.25	0.21	0.26	0.19	-0.04	0.01	-0.06
	59	0.18	0.29	0.35	0.30	0.11	0.17	0.12
	60	0.39	0.36	0.36	0.33	-0.03	-0.03	-0.06
	61	0.40	0.42	0.41	0.38	0.02	0.01	-0.02
	62	0.53	0.61	0.59	0.55	0.08	0.06	0.02
	63	0.53	0.61	0.59	0.56	0.08	0.06	0.03
	64	0.39	0.47	0.47	0.43	0.08	0.08	0.04
	65	0.28	0.38	0.37	0.34	0.10	0.09	0.06
	66	0.33	0.31	0.33	0.27	-0.02	0.00	-0.06
MAD (mm s^{-1})			**0.058**	**0.071**	**0.048**			

[a]SD = Signed Deviation= $[\delta_{cal} - \delta_{exp}]$/mm s^{-1}

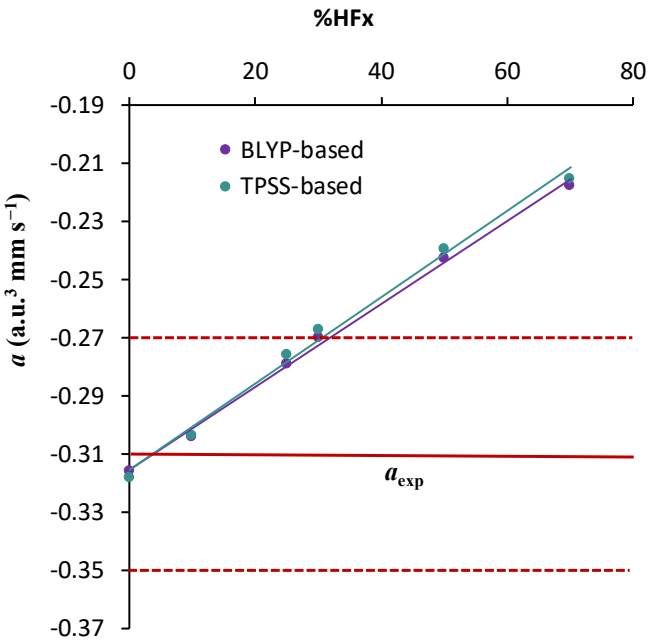

Figure S1: Effect of HF exchange on "*a*", obtained from linear regression analysis. The red solid line represents the experimental "*a*", and the dashed line are the upper and lower limit of "*a*" reported in Ref.[64] Color code: violet for the BLYP- and teal for the TPSS-based functionals.

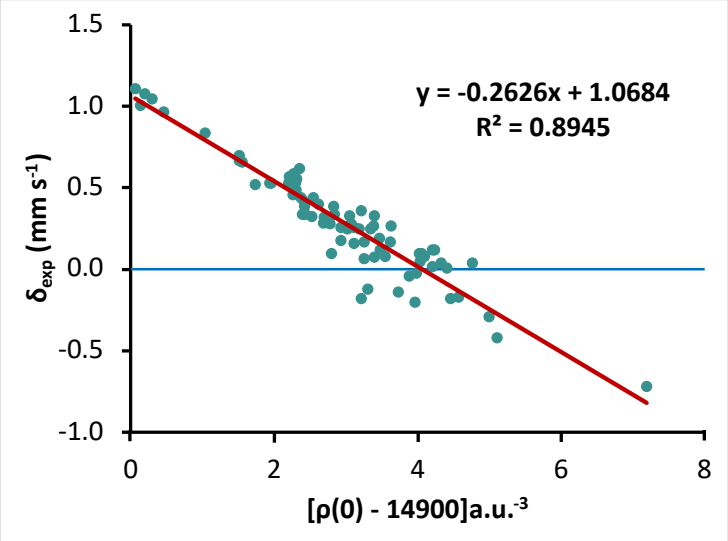

Figure S2: Linear fit of the DSD-PBEP86/*s*-decontracted aug-cc-pVTZ-J (Fe) + x2c-TZVPPall level contact densities against the experimental isomer shifts with relaxed PT2 density.

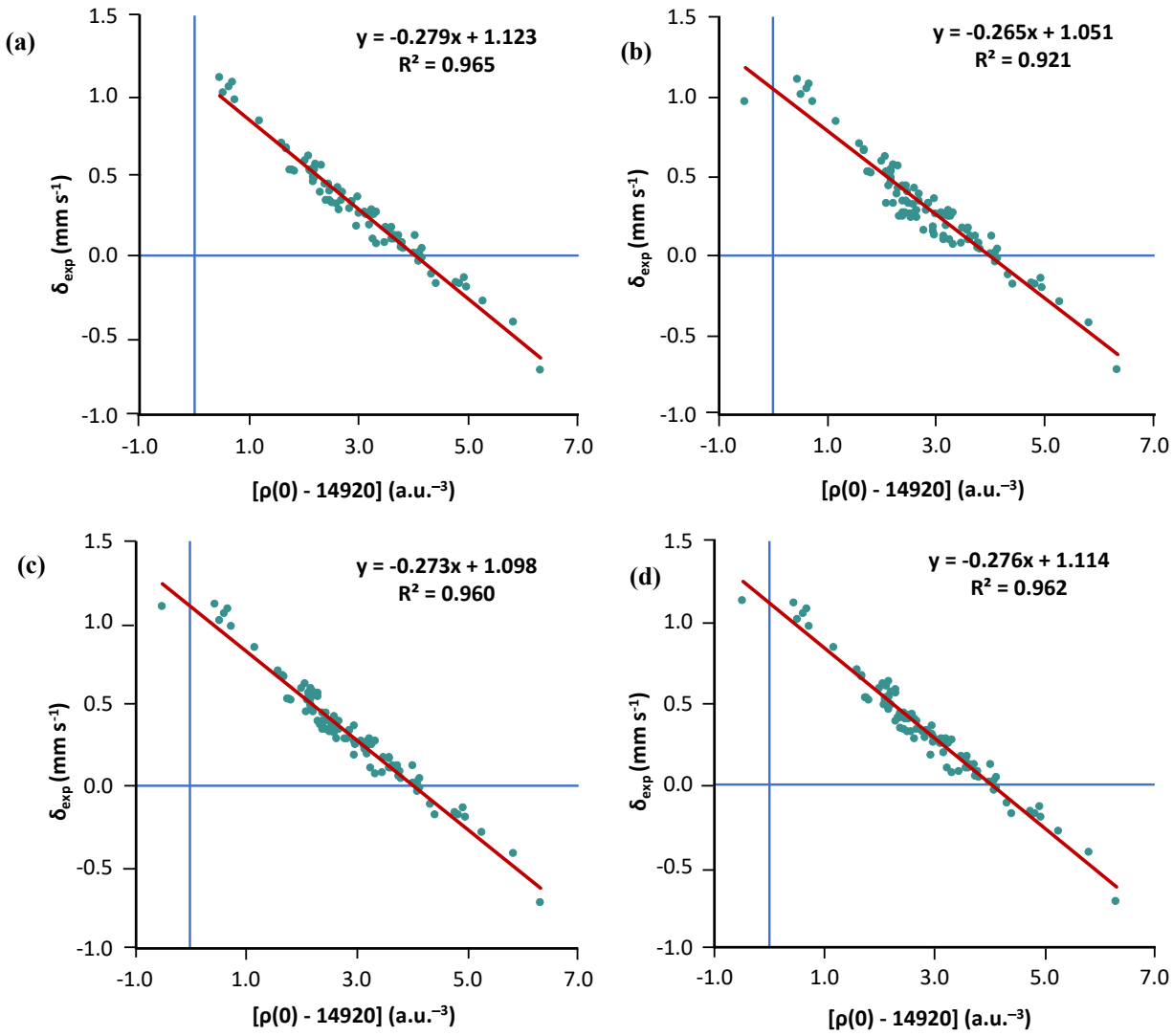

Figure S3: Linear fit of the calculated PBE0/*s*-decontracted aug-cc-pVTZ-J+x2c-TZVPPall level contact densities against the (a) low-T isomer shifts of MPMIC80; (b) 80 low-T and 21 high-T isomer shifts; (c) 80 low-T isomer shifts and 21 isomer shifts with Noodleman's high-T SODS correction (0.12 mm s^{-1})[65-68] and (d) 80 low-T isomer shifts and 21 isomer shifts with refitted high-T SODS correction (0.16 mm s^{-1}).

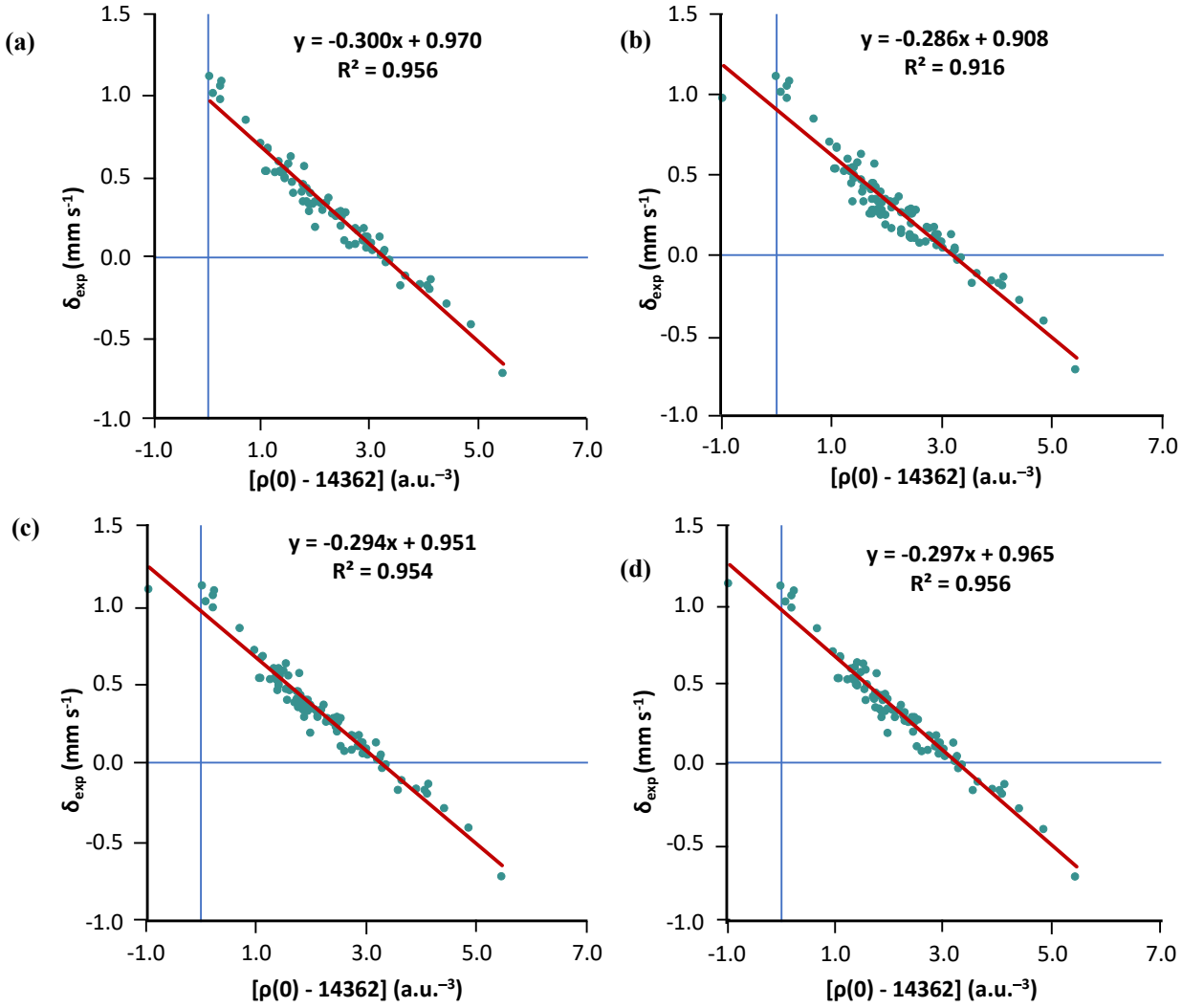

Figure S4: Linear fit of the calculated B3LYP/CP(PPP)+x2c-TZVPPall level contact densities against the (a) low-T isomer shifts of MPMIC80; (b) 80 low-T and 21 high-T isomer shifts; (c) 80 low-T isomer shifts and 21 isomer shifts with Noodleman's high-T SODS correction (0.12 mm s^{-1})[65-68] and (d) 80 low-T isomer shifts and 21 isomer shifts with refitted high-T SODS correction (0.16 mm s^{-1}).

(a)

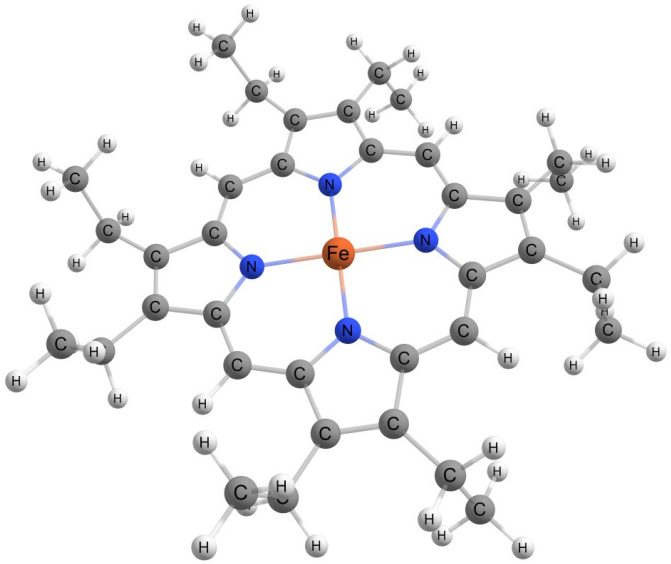

(b)

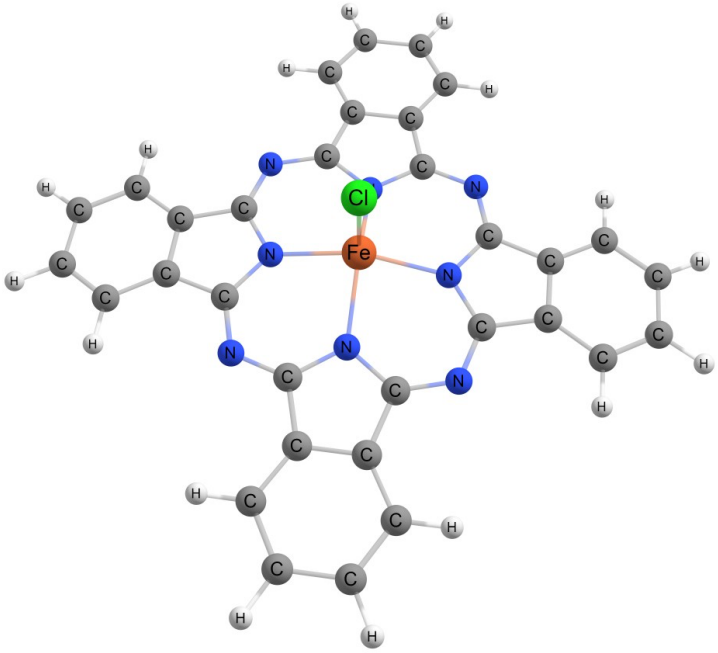

Figure S5: Structures of (a) iron(III) phthalocyanine chloride and (b) octaethylporphyrinato-iron(II).

ORCA Sample Inputs

A. Optimization

```
! TPSSh D3BJ RIJCOSX x2c/J x2c x2c-TZVPall DEFGRID2 TightSCF Opt
! PrintBasis PrintMOs

%rel
PictureChange 1
end

* xyzfile [Charge] [Multiplicity] [XYZFileName.xyz]
```

B. Mössbauer property calculation

TPSS0/*s*-decontracted aug-cc-pVTZ-J + x2c-TZVPPall

```
! UKS TPSS0 RIJCOSX x2c/J x2c x2c-TZVPPall PrintBasis DEFGRID3
! TightSCF NoPOP PrintMOs

%rel
PictureChange 1
FiniteNuc true
end

%basis
 NewGTO Fe
 S 1
   1  8584004113.0000000000      1.0000000000
 S 1
   1  1285418254.0000000000      1.0000000000
 S 1
   1  192485938.5000000000      1.0000000000
 S 1
   1  28823953.9100000001      1.0000000000
 S 1
   1  4316265.0000000000      1.0000000000
 S 1
   1  646342.4000000000      1.0000000000
 S 1
   1  147089.7000000000      1.0000000000
 S 1
   1   41661.5200000000      1.0000000000
 S 1
   1   13590.7700000000      1.0000000000
 S 1
   1    4905.7500000000      1.0000000000
 S 1
   1    1912.7460000000      1.0000000000
 S 1
   1     792.6043000000      1.0000000000
 S 1
   1     344.8065000000      1.0000000000
 S 1
```

```
  1     155.8999000000      1.0000000000
S 1
  1      72.2309100000      1.0000000000
S 1
  1      32.7250600000      1.0000000000
S 1
  1      15.6676200000      1.0000000000
S 1
  1       7.5034830000      1.0000000000
S 1
  1       3.3122230000      1.0000000000
S 1
  1       1.5584710000      1.0000000000
S 1
  1       0.6839140000      1.0000000000
S 1
  1       0.1467570000      1.0000000000
S 1
  1       0.0705830000      1.0000000000
S 1
  1       0.0314490000      1.0000000000
S 1
  1       0.0140100000      1.0000000000
P 10
  1   74965.5865200000     -0.0000030652
  2   17745.6900000000     -0.0000426385
  3    4200.7210000000     -0.0004353595
  4    1364.4290000000     -0.0023546474
  5     522.0806000000     -0.0109370575
  6     221.4595000000     -0.0379266480
  7     100.9096000000     -0.1071129611
  8      48.4011500000     -0.2385782781
  9      23.9853600000     -0.3765275830
 10      12.1825000000     -0.3753260135
P 10
  1   74965.5865200000     -0.0000026059
  2   17745.6900000000     -0.0000381329
  3    4200.7210000000     -0.0003782391
  4    1364.4290000000     -0.0021042401
  5     522.0806000000     -0.0096040490
  6     221.4595000000     -0.0344433334
  7     100.9096000000     -0.0978912053
  8      48.4011500000     -0.2337788211
  9      23.9853600000     -0.3706145174
 10      12.1825000000     -0.3955462688
P 1
  1       6.2422980000      1.0000000000
P 1
  1       3.1109440000      1.0000000000
P 1
  1       1.5099580000      1.0000000000
P 1
  1       0.7108450000      1.0000000000
P 1
  1       0.2731900000      1.0000000000
P 1
  1       0.1042330000      1.0000000000
P 1
  1       0.0382910000      1.0000000000
P 1
  1       0.0140700000      1.0000000000
```

```
 D 4
   1     381.8765668000     -0.0017960559
   2     113.3440000000     -0.0275628524
   3      33.6414000000     -0.2268797508
   4      12.3310000000     -0.8288676519
 D 1
   1       4.9947800000      1.0000000000
 D 1
   1       2.0728000000      1.0000000000
 D 1
   1       0.8307530000      1.0000000000
 D 1
   1       0.3091780000      1.0000000000
 D 1
   1       0.1001300000      1.0000000000
 D 1
   1       0.0324300000      1.0000000000
 F 1
   1       3.2758000000      1.0000000000
 F 1
   1       0.7920000000      1.0000000000
 F 1
   1       0.2749000000      1.0000000000
 G 1
   1       2.0897000000      1.0000000000
 G 1
   1       0.7871600000      1.0000000000
  end
end

* xyzfile [Charge] [Multiplicity] [XYZFileName.xyz]

%eprnmr
nuclei = all Fe { fgrad, rho}
end
```

Modified basis sets for iron

A. *s*-decontracted aug-cc-pVTZ-J

```
NewGTO Fe
 S 1
   1  8584004113.0000000000      1.0000000000
 S 1
   1  1285418254.0000000000      1.0000000000
 S 1
   1  192485938.5000000000      1.0000000000
 S 1
   1  28823953.9100000001      1.0000000000
 S 1
   1  4316265.0000000000      1.0000000000
 S 1
   1  646342.4000000000      1.0000000000
 S 1
   1  147089.7000000000      1.0000000000
 S 1
   1   41661.5200000000      1.0000000000
 S 1
   1   13590.7700000000      1.0000000000
 S 1
   1    4905.7500000000      1.0000000000
 S 1
   1    1912.7460000000      1.0000000000
 S 1
   1     792.6043000000      1.0000000000
 S 1
   1     344.8065000000      1.0000000000
 S 1
   1     155.8999000000      1.0000000000
 S 1
   1      72.2309100000      1.0000000000
 S 1
   1      32.7250600000      1.0000000000
 S 1
   1      15.6676200000      1.0000000000
 S 1
   1       7.5034830000      1.0000000000
 S 1
   1       3.3122230000      1.0000000000
 S 1
   1       1.5584710000      1.0000000000
 S 1
   1       0.6839140000      1.0000000000
 S 1
   1       0.1467570000      1.0000000000
 S 1
   1       0.0705830000      1.0000000000
 S 1
   1       0.0314490000      1.0000000000
 S 1
   1       0.0140100000      1.0000000000
 P 10
   1   74965.5865200000     -0.0000030652
   2   17745.6900000000     -0.0000426385
   3    4200.7210000000     -0.0004353595
   4    1364.4290000000     -0.0023546474
```

```
  5     522.0806000000     -0.0109370575
  6     221.4595000000     -0.0379266480
  7     100.9096000000     -0.1071129611
  8      48.4011500000     -0.2385782781
  9      23.9853600000     -0.3765275830
 10      12.1825000000     -0.3753260135
P 10
  1   74965.5865200000     -0.0000026059
  2   17745.6900000000     -0.0000381329
  3    4200.7210000000     -0.0003782391
  4    1364.4290000000     -0.0021042401
  5     522.0806000000     -0.0096040490
  6     221.4595000000     -0.0344433334
  7     100.9096000000     -0.0978912053
  8      48.4011500000     -0.2337788211
  9      23.9853600000     -0.3706145174
 10      12.1825000000     -0.3955462688
P 1
  1       6.2422980000      1.0000000000
P 1
  1       3.1109440000      1.0000000000
P 1
  1       1.5099580000      1.0000000000
P 1
  1       0.7108450000      1.0000000000
P 1
  1       0.2731900000      1.0000000000
P 1
  1       0.1042330000      1.0000000000
P 1
  1       0.0382910000      1.0000000000
P 1
  1       0.0140700000      1.0000000000
D 4
  1     381.8765668000     -0.0017960559
  2     113.3440000000     -0.0275628524
  3      33.6414000000     -0.2268797508
  4      12.3310000000     -0.8288676519
D 1
  1       4.9947800000      1.0000000000
D 1
  1       2.0728000000      1.0000000000
D 1
  1       0.8307530000      1.0000000000
D 1
  1       0.3091780000      1.0000000000
D 1
  1       0.1001300000      1.0000000000
D 1
  1       0.0324300000      1.0000000000
F 1
  1       3.2758000000      1.0000000000
F 1
  1       0.7920000000      1.0000000000
F 1
  1       0.2749000000      1.0000000000
G 1
  1       2.0897000000      1.0000000000
G 1
  1       0.7871600000      1.0000000000
 end
```

B. *s*-decontracted DKH-def2-TZVPP

```
NewGTO Fe
 S 1
   1  300784.8463700000      1.0000000000
 S 1
   1   45088.9705570000      1.0000000000
 S 1
   1   10262.5163170000      1.0000000000
 S 1
   1    2905.2897293000      1.0000000000
 S 1
   1     946.1148713700      1.0000000000
 S 1
   1     339.8783289400      1.0000000000
 S 1
   1     131.9442558800      1.0000000000
 S 1
   1      52.1114940800      1.0000000000
 S 1
   1     329.4883926700      1.0000000000
 S 1
   1     101.9233273900      1.0000000000
 S 1
   1      16.2404627400      1.0000000000
 S 1
   1       6.8840675800      1.0000000000
 S 1
   1      10.4706937800      1.0000000000
 S 1
   1       1.7360039600      1.0000000000
 S 1
   1       0.7257728900      1.0000000000
 S 1
   1       0.1159552800      1.0000000000
 S 1
   1       0.0419682300      1.0000000000
 P 6
   1    1585.3959970000      0.0034932434
   2     375.3800649900      0.0239178708
   3     120.3181650100      0.1064723133
   4      44.7887490300      0.3000149937
   5      17.8292785800      0.4790319948
   6       7.2247153800      0.2711928303
 P 1
   1      28.1432197600      1.0000000000
 P 1
   1       3.8743241400      1.0000000000
 P 1
   1       1.5410752300      1.0000000000
 P 1
   1       0.5828561500      1.0000000000
 D 4
   1      61.9966750300      0.0197602677
   2      17.8737325500      0.1191944039
   3       6.2744782900      0.3757301498
   4       2.3552337200      0.6504527363
 D 1
   1       0.8543224000      1.0000000000
```

```
 D 1
   1       0.2786925400      1.0000000000
 P 1
   1       0.2204000000      1.0000000000
 P 1
   1       0.0833800000      1.0000000000
 D 1
   1       0.0910000000      1.0000000000
 F 1
   1       3.4650000000      1.0000000000
 F 1
   1       0.8430000000      1.0000000000
 G 1
   1       2.1280000000      1.0000000000
  end
```

C. *s*-decontracted x2c-TZVPPall

```
NewGTO Fe
 S 1
   1  568671.5851900000      1.0000000000
 S 1
   1   71381.6928490000      1.0000000000
 S 1
   1   14484.2693160000      1.0000000000
 S 1
   1    3781.8649758000      1.0000000000
 S 1
   1    1159.5814022000      1.0000000000
 S 1
   1     398.0167732600      1.0000000000
 S 1
   1     147.9728740800      1.0000000000
 S 1
   1      56.1872993440      1.0000000000
 S 1
   1     348.2904042700     1.0000000000
 S 1
   1     105.8462345400     1.0000000000
 S 1
   1      16.8387194490      1.0000000000
 S 1
   1       7.1130781143      1.0000000000
 S 1
   1      10.7323618120     1.0000000000
 S 1
   1       1.7765872891      1.0000000000
 S 1
   1       0.7462990075      1.0000000000
 S 1
   1       0.1195431489      1.0000000000
 S 1
   1       0.0431448968      1.0000000000
 P 6
   1    1913.6765901000      0.0027108020
   2     421.5599419000      0.0206883282
   3     130.4737972700      0.0979285981
   4      47.5111355840      0.2895413458
   5      18.5993994750      0.4814264752
   6       7.4496187612      0.2916698170
```

```
 P 3
   1      28.6053607740     -0.0197461280
   2       3.9427871862      0.3813687711
   3       1.5699529988      0.6794911301
 P 1
   1       0.5929839866      1.0000000000
 D 4
   1      64.1204517710      0.0187699309
   2      18.3894986480      0.1158182891
   3       6.4193601128      0.3727830763
   4       2.3965919355      0.6564490493
 D 1
   1       0.8637471259      1.0000000000
 D 1
   1       0.2795554046      1.0000000000
 P 1
   1       0.2204000000      1.0000000000
 P 1
   1       0.0833800000      1.0000000000
 D 1
   1       0.0910000000      1.0000000000
 F 1
   1       3.4650000000      1.0000000000
 F 1
   1       0.8430000000      1.0000000000
 G 1
   1       2.1280000000      1.0000000000
  end
```

D. *s*-decontracted aug-cc-pVTZ-J(-*dfg*)

```
NewGTO Fe
 S 1
   1  8584004113.0000000000      1.0000000000
 S 1
   1  1285418254.0000000000      1.0000000000
 S 1
   1  192485938.5000000000      1.0000000000
 S 1
   1  28823953.9100000001      1.0000000000
 S 1
   1  4316265.0000000000      1.0000000000
 S 1
   1  646342.4000000000      1.0000000000
 S 1
   1  147089.7000000000      1.0000000000
 S 1
   1   41661.5200000000      1.0000000000
 S 1
   1   13590.7700000000      1.0000000000
 S 1
   1    4905.7500000000      1.0000000000
 S 1
   1    1912.7460000000      1.0000000000
 S 1
   1     792.6043000000      1.0000000000
 S 1
   1     344.8065000000      1.0000000000
 S 1
   1     155.8999000000      1.0000000000
```

```
S 1
  1      72.2309100000      1.0000000000
S 1
  1      32.7250600000      1.0000000000
S 1
  1      15.6676200000      1.0000000000
S 1
  1       7.5034830000      1.0000000000
S 1
  1       3.3122230000      1.0000000000
S 1
  1       1.5584710000      1.0000000000
S 1
  1       0.6839140000      1.0000000000
S 1
  1       0.1467570000      1.0000000000
S 1
  1       0.0705830000      1.0000000000
S 1
  1       0.0314490000      1.0000000000
S 1
  1       0.0140100000      1.0000000000
P 10
  1   74965.5865200000     -0.0000030652
  2   17745.6900000000     -0.0000426385
  3    4200.7210000000     -0.0004353595
  4    1364.4290000000     -0.0023546474
  5     522.0806000000     -0.0109370575
  6     221.4595000000     -0.0379266480
  7     100.9096000000     -0.1071129611
  8      48.4011500000     -0.2385782781
  9      23.9853600000     -0.3765275830
 10      12.1825000000     -0.3753260135
P 10
  1   74965.5865200000     -0.0000026059
  2   17745.6900000000     -0.0000381329
  3    4200.7210000000     -0.0003782391
  4    1364.4290000000     -0.0021042401
  5     522.0806000000     -0.0096040490
  6     221.4595000000     -0.0344433334
  7     100.9096000000     -0.0978912053
  8      48.4011500000     -0.2337788211
  9      23.9853600000     -0.3706145174
 10      12.1825000000     -0.3955462688
P 1
  1       6.2422980000      1.0000000000
P 1
  1       3.1109440000      1.0000000000
P 1
  1       1.5099580000      1.0000000000
P 1
  1       0.7108450000      1.0000000000
P 1
  1       0.2731900000      1.0000000000
P 1
  1       0.1042330000      1.0000000000
P 1
  1       0.0382910000      1.0000000000
P 1
  1       0.0140700000      1.0000000000
D 4
```

```
   1     381.8765668000     -0.0017960559
   2     113.3440000000     -0.0275628524
   3      33.6414000000     -0.2268797508
   4      12.3310000000     -0.8288676519
 D 1
   1       4.9947800000      1.0000000000
 D 1
   1       2.0728000000      1.0000000000
 D 1
   1       0.8307530000      1.0000000000
 D 1
   1       0.3091780000      1.0000000000
 D 1
   1       0.1001300000      1.0000000000
 F 1
   1       3.2758000000      1.0000000000
 F 1
   1       0.7920000000      1.0000000000
 G 1
   1       2.0897000000      1.0000000000
  end
```

E. aug-cc-pVTZ-Jmod

Proposed by Pantazis and co-workers for calculations of core properties.[63]

```
NewGTO Fe
 S 1
   1  28823953.9100000001      1.0000000000
 S 1
   1  4316265.0000000000      1.0000000000
 S 1
   1  646342.4000000000      1.0000000000
 S 1
   1  147089.7000000000      1.0000000000
 S 1
   1   41661.5200000000      1.0000000000
 S 1
   1   13590.7700000000      1.0000000000
 S 1
   1    4905.7500000000      1.0000000000
 S 1
   1    1912.7460000000      1.0000000000
 S 1
   1     792.6043000000      1.0000000000
 S 1
   1     344.8065000000      1.0000000000
 S 1
   1     155.8999000000      1.0000000000
 S 1
   1      72.2309100000      1.0000000000
 S 1
   1      32.7250600000      1.0000000000
 S 1
   1      15.6676200000      1.0000000000
 S 1
   1       7.5034830000      1.0000000000
 S 1
   1       3.3122230000      1.0000000000
```

```
S 1
  1       1.5584710000      1.0000000000
S 1
  1       0.6839140000      1.0000000000
S 1
  1       0.1467570000      1.0000000000
S 1
  1       0.0705830000      1.0000000000
S 1
  1       0.0314490000      1.0000000000
S 1
  1       0.0140100000      1.0000000000
P 10
  1   74965.5865200000     -0.0000030652
  2   17745.6900000000     -0.0000426385
  3    4200.7210000000     -0.0004353595
  4    1364.4290000000     -0.0023546474
  5     522.0806000000     -0.0109370575
  6     221.4595000000     -0.0379266480
  7     100.9096000000     -0.1071129611
  8      48.4011500000     -0.2385782781
  9      23.9853600000     -0.3765275830
 10      12.1825000000     -0.3753260135
P 10
  1   74965.5865200000     -0.0000026059
  2   17745.6900000000     -0.0000381329
  3    4200.7210000000     -0.0003782391
  4    1364.4290000000     -0.0021042401
  5     522.0806000000     -0.0096040490
  6     221.4595000000     -0.0344433334
  7     100.9096000000     -0.0978912053
  8      48.4011500000     -0.2337788211
  9      23.9853600000     -0.3706145174
 10      12.1825000000     -0.3955462688
P 1
  1       6.2422980000      1.0000000000
P 1
  1       3.1109440000      1.0000000000
P 1
  1       1.5099580000      1.0000000000
P 1
  1       0.7108450000      1.0000000000
P 1
  1       0.2731900000      1.0000000000
P 1
  1       0.1042330000      1.0000000000
P 1
  1       0.0382910000      1.0000000000
P 1
  1       0.0140700000      1.0000000000
D 4
  1     381.8765668000     -0.0017960559
  2     113.3440000000     -0.0275628524
  3      33.6414000000     -0.2268797508
  4      12.3310000000     -0.8288676519
D 1
  1       4.9947800000      1.0000000000
D 1
  1       2.0728000000      1.0000000000
D 1
  1       0.8307530000      1.0000000000
```

```
D 1
  1        0.3091780000      1.0000000000
D 1
  1        0.1001300000      1.0000000000
D 1
  1        0.0324300000      1.0000000000
F 1
  1        3.2758000000      1.0000000000
F 1
  1        0.7920000000      1.0000000000
F 1
  1        0.2749000000      1.0000000000
G 1
  1        2.0897000000      1.0000000000
G 1
  1        0.7871600000      1.0000000000
 end
```

References

1. R. Greatrex and N. Greenwood, Mössbauer spectra, structure, and bonding in iron carbonyl derivatives, *Discuss. Faraday Soc.*, 1969, **47**, 126-135.
2. W. Kerler, W. Neuwirth and E. Fluck, Isomerieverschiebung und Quadrupolaufspaltung beim Mößbauer-Effekt von Fe^{57} in Eisenverbindungen, *Z. Phys.*, 1963, **175**, 200-220.
3. Y. Yamada and T. Tominaga, Molecular orbital calculation of Mössbauer parameters for iron carbonyl compounds isolated in low temperature matrices, *Radiochim. Acta*, 1998, **80**, 163-170.
4. S. Kukolich, M. Roehrig, D. Wallace and G. Henderson, Microwave measurements of the rotational spectrum and structure of butadieneiron tricarbonyl, *J. Am. Chem. Soc.*, 1993, **115**, 2021-2027.
5. E. I. Solomon and A. B. P. Lever, *Inorganic electronic structure and spectroscopy*, Wiley, New York, 1999.
6. S. F. McWilliams, E. Brennan-Wydra, K. C. MacLeod and P. L. Holland, Density Functional Calculations for Prediction of ^{57}Fe Mössbauer Isomer Shifts and Quadrupole Splittings in β-Diketiminate Complexes, *ACS Omega*, 2017, **2**, 2594-2606.
7. E. Koenig and K. Madeja, 5T2-1A1 Equilibriums in some iron (II)-bis (1, 10-phenanthroline) complexes, *Inorg. Chem.*, 1967, **6**, 48-55.
8. I. Dézsi, B. Molnar, T. Tarnoczi and K. Tompa, On the magnetic behaviour of iron (II)-bis-(1, 10 phenantroline)-thiocyanate between− 190° and 30° C, *J. Inorg. Nucl. Chem.*, 1967, **29**, 2486-2490.
9. N. Bréfuel, I. Vang, S. Shova, F. Dahan, J.-P. Costes and J.-P. Tuchagues, FeII Spin crossover materials based on dissymmetrical N4 Schiff bases including 2-pyridyl and 2R-imidazol-4-yl rings: Synthesis, crystal structure and magnetic and Mössbauer properties, *Polyhedron*, 2007, **26**, 1745-1757.
10. E. Fluck, in *Chemical Applications of Mössbauer Spectroscopy*, eds. V. I. Goldanskii and R. H. Herber, Academic Press, Inc.: New York, 1968, pp. 268– 311.
11. M. Li, D. Bonnet, E. Bill, F. Neese, T. Weyhermüller, N. Blum, D. Sellmann and K. Wieghardt, Tuning the Electronic Structure of Octahedral Iron Complexes [FeL (X)](L= 1-Alkyl-4, 7-bis (4-tert-butyl-2-mercaptobenzyl)-1, 4, 7-triazacyclononane, X= Cl, CH_3O, CN, NO). The S= 1/2⇌ S= 3/2 Spin Equilibrium of [FeLPr (NO)], *Inorg. Chem.*, 2002, **41**, 3444-3456.
12. R. H. Havlin, N. Godbout, R. Salzmann, M. Wojdelski, W. Arnold, C. E. Schulz and E. Oldfield, An experimental and density functional theoretical investigation of iron-57 Mössbauer quadrupole splittings in organometallic and heme-model compounds: applications to carbonmonoxy-heme protein structure, *J. Am. Chem. Soc.*, 1998, **120**, 3144-3151.
13. N. J. Silvernail, B. C. Noll, C. E. Schulz and W. R. Scheidt, Coordination of diatomic ligands to heme: Simply CO, *Inorg. Chem.*, 2006, **45**, 7050-7052.
14. B. V. Obrist, D. Chen, A. Ahrens, V. Schünemann, R. Scopelliti and X. Hu, An iron carbonyl pyridonate complex related to the active site of the [Fe]-hydrogenase (Hmd), *Inorg. Chem.*, 2009, **48**, 3514-3516.
15. D. Chen, A. Ahrens-Botzong, V. Schünemann, R. Scopelliti and X. Hu, Synthesis and characterization of a series of model complexes of the active site of [Fe]-hydrogenase (Hmd), *Inorg. Chem.*, 2011, **50**, 5249-5257.
16. P. E. Gütlich, J, in *Inorganic electronic structure and spectroscopy*, ed. A. B. P. S. Lever, E. I., John Wiley and Sons: New York, 1999, vol. 1, pp. 161– 212.
17. M. Garcia Posse, M. Juri, P. Aymonino, O. Piro, H. Negri and E. Castellano, Additions and Corrections-Synthesis, Crystal and Molecular Structure, and Spectroscopic Properties of Tris (2, 2'-bipyridyl) iron (II) Nitroprusside Tetrahydrate $[Fe(bpy)_3][Fe(CN)_5NO]$-$4H_2O$, *Inorg. Chem.*, 1984, **23**, 1788-1788.
18. W. M. Reiff, E. H. Witten, K. Mottle, T. F. Brennan and A. R. Garafalo, The ferric chloride α-di-imine system. Part V. X-ray structure determination of tris(1,10-phenanthroline)iron(II)μ-oxo-bis(trichloroiron(III)·DMF, *Inorg. Chim. Acta*, 1983, **77**, L83-L88.

19. D. L. Reger, C. A. Little, M. D. Smith, A. L. Rheingold, K. C. Lam, T. L. Concolino, G. J. Long, R. P. Hermann and F. Grandjean, Synthetic, structural, magnetic, and Mössbauer spectral study of {Fe [HC (3, 5-$Me_2pz)_3]_2$}I_2 and its spin-state crossover behavior, *Eur. J. Inorg. Chem.*, 2002, **2002**, 1190-1197.

20. R. A. Stukan, S. P. Gubin, A. N. Nesmeyanov, V. I. Gol'danskii and E. F. Makarov, A Mössbauer study of some ferrocene derivatives, *Theor. Exp. Chem.*, 1966, **2**, 581-584.

21. M. Hanack, U. Keppeler, A. Lange, A. Hirsch and R. Dieing, in *Phthalocyanines: Properties and Applications*, eds. A. B. P. Lever and C. C. Leznoff, Wiley-VCH: New York, 1993, vol. 2, p. 43−96.

22. M. Keilwerth, W. Mao, S. A. V. Jannuzzi, L. Grunwald, F. W. Heinemann, A. Scheurer, J. Sutter, S. DeBeer, D. Munz and K. Meyer, From Divalent to Pentavalent Iron Imido Complexes and an Fe(V) Nitride via N–C Bond Cleavage, *J. Am. Chem. Soc.*, 2023, **145**, 873-887.

23. H. Schottenberger, M. R. Buchmeiser and R. H. Herber, ^{57}Fe-Mössbauer spectroscopic study of monomeric and polymeric ferrocenyl- and octamethylferrocenyl-substituted ethynes, *J. Organomet. Chem.*, 2000, **612**, 1-8.

24. S. H. Strauss, M. E. Silver, K. M. Long, R. G. Thompson, R. A. Hudgens, K. Spartalian and J. A. Ibers, Comparison of the molecular and electronic structures of (2,3,7,8,12,13,17,18-octaethylporphyrinato)iron(II) and (trans-7,8-dihydro-2,3,7,8,12,13,17,18-octaethylporphyrinato)iron(II), *J. Am. Chem. Soc.*, 1985, **107**, 4207-4215.

25. J. P. Collman, J. L. Hoard, N. Kim, G. Lang and C. A. Reed, Synthesis, stereochemistry, and structure-related properties of .alpha.,.beta.,.gamma.,.delta.-tetraphenylporphinatoiron(II), *J. Am. Chem. Soc.*, 1975, **97**, 2676-2681.

26. N. Li, Z. Su, P. Coppens and J. Landrum, X-ray diffraction study of the electronic ground state of (meso-tetraphenylporphinato)iron(II), *J. Am. Chem. Soc.*, 1990, **112**, 7294-7298.

27. Y. Huang, M.-E. Moret, R. J. M. Klein Gebbink and M. Lutz, Crystallographic Space Group Choice and Its Chemical Consequences: Revised Crystal Structure of $[Fe(phen)_2Cl_2]NO_3$, *Eur. J. Inorg. Chem.*, 2013, **2013**, 2467-2469.

28. D. Coucouvanis, D. Swenson, N. Baenziger, C. Murphy, D. Holah, N. Sfarnas, A. Simopoulos and A. Kostikas, Tetrahedral complexes containing the Fe (II) S4 core. The syntheses, ground-state electronic structures and crystal and molecular structures of the bis (tetraphenylphosphonium) tetrakis (thiophenolato) ferrate (II) and bis (tetrapheny lphosphonium) bis (dithiosquarato) ferrate (II) complexes. An analog for the active site in reducd rubredoxins (Rdred), *J. Am. Chem. Soc.*, 1981, **103**, 3350-3362.

29. P. R. Edwards, C. E. Johnson and R. J. P. Williams, Mössbauer Spectra of Some Tetrahedral Iron (II) Compounds, *J. Chem. Phys.*, 2004, **47**, 2074-2082.

30. Y. Sanakis, P. P. Power, A. Stubna and E. Münck, Mössbauer Study of the Three-Coordinate Planar FeII Thiolate Complex $[Fe(SR)_3]$-(R=C_6H_2-2, 4, 6-tBu_3): Model for the Trigonal Iron Sites of the MoFe7S9: Homocitrate Cofactor of Nitrogenase, *Inorg. Chem.*, 2002, **41**, 2690-2696.

31. F. M. MacDonnell, K. Ruhlandt-Senge, J. J. Ellison, R. Holm and P. P. Power, Sterically encumbered iron (II) thiolate complexes: synthesis and structure of trigonal planar [Fe (SR) 3]-(R= 2, 4, 6-t-Bu3C6H2) and Mössbauer spectra of two-and three-coordinate complexes, *Inorg. Chem.*, 1995, **34**, 1815-1822.

32. E. L. Bominaar, X. Q. Ding, A. Gismelseed, E. Bill, H. Winkler, A. X. Trautwein, H. Nasri, J. Fischer and R. Weiss, Structural, Moessbauer, and EPR investigations on two oxidation states of a five-coordinate, high-spin synthetic heme. Quantitative interpretation of zero-field parameters and large quadrupole splitting, *Inorg. Chem.*, 1992, **31**, 1845-1854.

33. K. C. MacLeod, S. F. McWilliams, B. Q. Mercado and P. L. Holland, Stepwise N–H bond formation from N_2-derived iron nitride, imide and amide intermediates to ammonia, *Chem. Sci.*, 2016, **7**, 5736-5746.

34. M. Garcia Posse, M. Juri, P. Aymonino, O. Piro, H. Negri and E. Castellano, Additions and Corrections-Synthesis, Crystal and Molecular Structure, and Spectroscopic Properties of Tris (2, 2'-bipyridyl) iron (II) Nitroprusside Tetrahydrate [Fe (bpy) 3][Fe (CN) 5NO]-4H2O, *Inorg. Chem.*, 1984, **23**, 1788-1788.

35. L. A. Barrios, C. Bartual-Murgui, E. Peyrecave-Lleixà, B. Le Guennic, S. J. Teat, O. Roubeau and G. Aromí, Homoleptic versus Heteroleptic Formation of Mononuclear Fe(II) Complexes with Tris-Imine Ligands, *Inorg. Chem.*, 2016, **55**, 4110-4116.

36. H. Oshio, H. Spiering, V. Ksenofontov, F. Renz and P. Gütlich, Electronic Relaxation Phenomena Following 57Co(EC)57Fe Nuclear Decay in [MnII(terpy)2](ClO4)2·1/2H2O and in the Spin Crossover Complexes [CoII(terpy)2]X2·nH2O (X = Cl and ClO4): A Mössbauer Emission Spectroscopic Study, *Inorg. Chem.*, 2001, **40**, 1143-1150.

37. K. Meyer, E. Bill, B. Mienert, T. Weyhermüller and K. Wieghardt, Photolysis of cis- and trans-$[FeIII(cyclam)(N_3)_2]^+$ Complexes: Spectroscopic Characterization of a Nitridoiron(V) Species, *J. Am. Chem. Soc.*, 1999, **121**, 4859-4876.

38. M. K. Safo, G. P. Gupta, F. A. Walker and W. R. Scheidt, Models of the cytochromes b. Control of axial ligand orientation with a hindered porphyrin system, *J. Am. Chem. Soc.*, 1991, **113**, 5497-5510.

39. Y. Maeda, H. Oshio, Y. Takashima, M. Mikuriya and M. Hidaka, Crystal structure, Moessbauer spectra, and magnetic properties of bis [N-(1-acetyl-2-propylidene)(2-pyridylmethyl) aminato] iron (1+) hexafluorophosphate and crystallographic changes in fast electronic relaxation between S= 1/2 and S= 5/2, *Inorg. Chem.*, 1986, **25**, 2958-2962.

40. S. Hayami, K. Hashiguchi, K. Inoue and Y. Maeda, Photo-induced spin transition for an iron (III) pyruvic acid thiosemicarbazone compound, *J. Nucl. Radiochem. Sci.*, 2004, **5**, N1-N3.

41. M. Malischewski, K. Seppelt, J. Sutter, D. Munz and K. Meyer, A Ferrocene-Based Dicationic Iron(IV) Carbonyl Complex, *Angew. Chem., Int. Ed.*, 2018, **57**, 14597-14601.

42. M. Fettouhi, M. Morsy, A. Waheed, S. Golhen, L. Ouahab, J.-P. Sutter, O. Kahn, N. Menendez and F. Varret, Spin-Crossover in the Complex Bis (cis-1, 2-dicyano-1, 2-ethylenedithiolato)[2-(p-pyridyl)-4, 4, 5, 5-tetramethylimidazolinium] iron (III), *Inorg. Chem.*, 1999, **38**, 4910-4912.

43. K. L. Kostka, B. G. Fox, M. P. Hendrich, T. J. Collins, C. E. Rickard, L. J. Wright and E. Munck, High-valent transition metal chemistry. Moessbauer and EPR studies of high-spin (S= 2) iron (IV) and intermediate-spin (S= 3/2) iron (III) complexes with a macrocyclic tetraamido-N ligand, *J. Am. Chem. Soc.*, 1993, **115**, 6746-6757.

44. T. C. Harrop, D. Song and S. J. Lippard, Interaction of nitric oxide with tetrathiolato iron (II) complexes: relevance to the reaction pathways of iron nitrosyls in sulfur-rich biological coordination environments, *J. Am. Chem. Soc.*, 2006, **128**, 3528-3529.

45. L. E. Maelia, M. Millar and S. A. Koch, General synthesis of iron (III) tetrathiolate complexes. Structural and spectroscopic models for the $[Fe(Cys\text{-}S)_4]$ center in oxidized rubredoxin, *Inorg. Chem.*, 1992, **31**, 4594-4600.

46. T. C. Harrop, Z. J. Tonzetich, E. Reisner and S. J. Lippard, Reactions of synthetic [2Fe-2S] and [4Fe-4S] clusters with nitric oxide and nitrosothiols, *J. Am. Chem. Soc.*, 2008, **130**, 15602-15610.

47. Y. Ohgo, S. Neya, T. Ikeue, N. Funasaki and M. Nakamura, Chloro(3,6,13,16-tetraethyl-2,7,12,17-tetramethylporphycenato-[kappa]4N)iron(III) chloroform solvate, *Acta Crystallogr. C*, 2001, **57**, 1046-1047.

48. E. L. Bominaar, X. Q. Ding, A. Gismelseed, E. Bill, H. Winkler, A. X. Trautwein, H. Nasri, J. Fischer and R. Weiss, Structural, Mössbauer, and EPR investigations on two oxidation states of a five-coordinate, high-spin synthetic heme. Quantitative interpretation of zero-field parameters and large quadrupole splitting, *Inorg. Chem.*, 1992, **31**, 1845-1854.

49. V. Varnek, I. Igumenov, P. Stabnikov and L. Mazalov, Parameters and Form of the Mössbauer Spectra of Iron (III) β-Diketonates: New Data, *J. Struct. Chem.*, 2000, **41**, 977-988.

50. M. M. Rodriguez, E. Bill, W. W. Brennessel and P. L. Holland, N2 reduction and hydrogenation to ammonia by a molecular iron-potassium complex, *Science*, 2011, **334**, 780-783.

51. C. Souilah, S. A. V. Jannuzzi, D. Demirbas, S. Ivlev, M. Swart, S. DeBeer and A. Casitas, Synthesis of FeIII and FeIV Cyanide Complexes Using Hypervalent Iodine Reagents as Cyano-Transfer One-Electron Oxidants, *Angew. Chem., Int. Ed.*, 2022, **61**, e202201699.

52. D. Sellmann, M. Geck, F. Knoch, G. Ritter and J. Dengler, Transition-metal complexes with sulfur ligands. 57. Stabilization of high-valent iron (IV) centers and vacant coordination sites by sulfur. pi.-donation: syntheses, x-ray structures, and properties of [Fe (" S2") 2 (PMe3) n](n= 1, 2) and (NMe4)[Fe

(" S2") 2 (PMe3) 2]. cntdot. CH3OH (" S2" 2-= 1, 2-benzenedithiolate (2-)), *J. Am. Chem. Soc.*, 1991, **113**, 3819-3828.

53. E. J. Klinker, J. Kaizer, W. W. Brennessel, N. L. Woodrum, C. J. Cramer and L. Que Jr., Structures of Nonheme Oxoiron(IV) Complexes from X-ray Crystallography, NMR Spectroscopy, and DFT Calculations, *Angew. Chem., Int. Ed.*, 2005, **44**, 3690-3694.

54. J.-U. Rohde, J.-H. In, M. H. Lim, W. W. Brennessel, M. R. Bukowski, A. Stubna, E. Münck, W. Nam and L. Que, Crystallographic and Spectroscopic Characterization of a Nonheme Fe(IV)=O Complex, *Science*, 2003, **299**, 1037-1039.

55. D. Mandon, R. Weiss, K. Jayaraj, A. Gold, J. Terner, E. Bill and A. Trautwein, Models for peroxidase compound I: generation and spectroscopic characterization of new oxoferryl porphyrin. pi. cation radical species, *Inorg. Chem.*, 1992, **31**, 4404-4409.

56. T. J. Collins, K. L. Kostka, E. Munck and E. S. Uffelman, Stabilization of mononuclear five-coordinate iron(IV), *J. Am. Chem. Soc.*, 1990, **112**, 5637-5639.

57. F. T. De Oliveira, A. Chanda, D. Banerjee, X. Shan, S. Mondal, L. Que Jr, E. L. Bominaar, E. Münck and T. J. Collins, Chemical and spectroscopic evidence for an Fe^{V}-oxo complex, *Science*, 2007, **315**, 835-838.

58. C. A. Grapperhaus, B. Mienert, E. Bill, T. Weyhermüller and K. Wieghardt, Mononuclear (Nitrido)iron(V) and (Oxo)iron(IV) Complexes via Photolysis of [(cyclam-acetato)FeIII(N3)]+ and Ozonolysis of [(cyclam-acetato)$Fe^{III}(O_3SCF_3)]^+$ in Water/Acetone Mixtures, *Inorg. Chem.*, 2000, **39**, 5306-5317.

59. J. F. Berry, E. Bill, E. Bothe, T. Weyhermüller and K. Wieghardt, Octahedral Non-Heme Non-Oxo Fe(IV) Species Stabilized by a Redox-Innocent N-Methylated Cyclam−Acetate Ligand, *J. Am. Chem. Soc.*, 2005, **127**, 11550-11551.

60. M. Keilwerth, W. Mao, M. Malischewski, S. A. V. Jannuzzi, K. Breitwieser, F. W. Heinemann, A. Scheurer, S. DeBeer, D. Munz, E. Bill and K. Meyer, The synthesis and characterization of an iron(VII) nitrido complex, *Nat. Chem.*, 2024, **16**, 514-520.

61. V. N. Nemykin, D. E. Nevonen, L. S. Ferch, M. Shepit, D. E. Herbert and J. van Lierop, Accurate Prediction of Mössbauer Hyperfine Parameters in Bis-Axially Coordinated Iron(II) Phthalocyanines Using Density Functional Theory Calculations: A Story of a Single Orbital Revealed by Natural Bond Orbital Analysis, *Inorg. Chem.*, 2021, **60**, 3690-3706.

62. D. L. Reger, C. A. Little, M. D. Smith, A. L. Rheingold, K. C. Lam, T. L. Concolino, G. J. Long, R. P. Hermann and F. Grandjean, Synthetic, structural, magnetic, and Mössbauer spectral study of {Fe [HC (3, 5-Me2pz) 3] 2} I2 and its spin-state crossover behavior, *Eur. J. Inorg. Chem.*, 2002, **2002**, 1190-1197.

63. R. J. Gómez-Piñeiro, D. A. Pantazis and M. Orio, Comparison of Density Functional and Correlated Wave Function Methods for the Prediction of Cu(II) Hyperfine Coupling Constants, *ChemPhysChem*, 2020, **21**, 2667-2679.

64. J. Ladrière, A. Meykens, R. Coussement, M. Cogneau, M. Boge, P. Auric, R. Bouchez, A. Benabed and J. Godard, Isomer shift calibration of ^{57}Fe by life-time variations in the electron-capture decay of ^{52}Fe, *J. Phys. Colloques*, 1979, **40**, C2-20-C22-22.

65. T. Liu, T. Lovell, W.-G. Han and L. Noodleman, DFT Calculations of Isomer Shifts and Quadrupole Splitting Parameters in Synthetic Iron−Oxo Complexes: Applications to Methane Monooxygenase and Ribonucleotide Reductase, *Inorg. Chem.*, 2003, **42**, 5244-5251.

66. W.-G. Han, T. Liu, T. Lovell and L. Noodleman, DFT calculations of ^{57}Fe Mössbauer isomer shifts and quadrupole splittings for iron complexes in polar dielectric media: Applications to methane monooxygenase and ribonucleotide reductase, *J. Comput. Chem.*, 2006, **27**, 1292-1306.

67. W.-G. Han and L. Noodleman, Structural model studies for the high-valent intermediate Q of methane monooxygenase from broken-symmetry density functional calculations, *Inorg. Chim. Acta*, 2008, **361**, 973-986.

68. K. H. Hopmann, A. Ghosh and L. Noodleman, Density Functional Theory Calculations on Mössbauer Parameters of Nonheme Iron Nitrosyls, *Inorg. Chem.*, 2009, **48**, 9155-9165.